Skew Andreev reflection in ferromagnet/superconductor junctions

Andreas Costa, Alex Matos-Abiague, and Jaroslav Fabian

Skew Andreev reflection in ferromagnet/superconductor junctions

Andreas Costa,[1, *] Alex Matos-Abiague,[2] and Jaroslav Fabian[1]

[1]*Institute for Theoretical Physics, University of Regensburg, 93040 Regensburg, Germany*
[2]*Department of Physics and Astronomy, Wayne State University Detroit, Michigan 48201, USA*
(Dated: August 9, 2019)

Andreev reflection (AR) in ferromagnet/superconductor junctions is an indispensable spectroscopic tool for measuring spin polarization. We study theoretically how the presence of a thin semiconducting interface in such junctions, inducing Rashba and Dresselhaus spin-orbit coupling, modifies AR processes. The interface gives rise to a momentum- and spin-dependent scattering potential, making the AR probability strongly asymmetric with respect to the sign of the incident electrons' transverse momenta. This *skew AR* creates spatial charge carrier imbalances and transverse Hall currents in the ferromagnet. We show that the effect is giant, compared to the normal regime. We provide a quantitative analysis and a qualitative picture of this phenomenon, and finally show that skew AR also leads to a widely tunable transverse supercurrent response in the superconductor.

Introduction. Due to the extraordinary properties occurring at their interfaces, ferromagnet/superconductor (F/S) heterostructures attract considerable interest [1–3]. Such junctions might not only offer novel tools for controlling and measuring charge and spin currents, but might also bring new functionalities into spintronics devices.

While early efforts focused on detecting spin-polarized quasiparticles in superconductors via spin transport experiments [4–6], current progress in the rapidly growing field of superconducting spintronics [2] opened several promising perspectives, ranging from the observation of long spin lifetimes and giant magnetoresistance effects [7] to the generation and successful manipulation of superconducting spin currents [8–15]. But the interplay of magnetism and superconductivity gets even more interesting when spin-orbit coupling (SOC) of the Rashba [16] and/or Dresselhaus [17] type is present [18, 19]. Prominent examples are spin-triplet pairing mechanisms [1, 20–25], leading to long-range superconducting proximity effects [26–29], and Majorana states [26, 30–36], which are expected to form in superconducting proximity regions in the presence of SOC.

While SOC in bulk materials plays the key role for *intrinsic anomalous Hall effects* [37–41], recent theoretical studies [42–47] predicted that interfacial SOC in F/normal metal (N) tunnel junctions can give rise to *extrinsic tunneling anomalous Hall effects (TAHEs)* in the N, owing to spin-polarized *skew tunneling* of electrons through the interface. The unique scaling of the associated TAHE conductances could make the effect to a fundamental tool for identifying and characterizing interfacial SOC, and thus providing the input for tailoring systems that could, e.g., host Majoranas. Although first experiments on granular junctions [48] confirmed the predictions, the extremely small TAHE conductances remain one of the main obstacles. Sizable TAHE conductances require either interfacial barriers with large SOC, such as ferroelectric semiconductors (SCs) [47], or different junction compositions.

In this paper, we consider F/SC/S junctions, in which the N electrode is replaced by a S. We demonstrate that, analogously to the tunneling picture in the normal-conducting case, *skew reflection* [49] of spin-polarized carriers at the barrier leads to TAHEs in the F. Due to the presence of a S electrode, we distinguish two skew reflection processes: *skew specular reflection (SR) and skew Andreev reflection (AR)*. By formulating a qualitative physical picture including both processes, we assert that skew SR and skew AR can act together and significantly enhance the TAHE compared to all previously studied (normal) systems. Special attention must be paid to skew AR, which transfers Cooper pairs across the barrier into the S. The electrons forming one Cooper pair are thereby also subject to the proposed skew reflection mechanism. We discuss that the result is a *transverse supercurrent response*, initially deduced from a phenomenological Ginzburg-Landau treatment [50], *with widely tunable characteristics*. Both findings, relatively giant TAHE conductances in the F and transverse supercurrents in the S, are distinct fingerprints to experimentally detect skew AR and characterize the junctions' interfacial SOC.

Theoretical model. We consider a biased ballistic F/SC/S junction grown along the $\hat{z}$-direction, in which the two semi-infinite F and S regions are separated by an ultrathin SC barrier; see Fig. 1(a). The barrier may be composed of a thin layer of zincblende materials (e.g., GaAs or InAs) and introduces potential scattering, as well as strong interfacial Rashba [16] and Dresselhaus [17] SOC [18, 19].

The system can be modeled by means of the stationary Bogoljubov–de Gennes (BdG) Hamiltonian [51],

$$\hat{\mathcal{H}}_{\mathrm{BdG}} = \begin{bmatrix} \hat{\mathcal{H}}_{\mathrm{e}} & \hat{\Delta}_{\mathrm{S}}(z) \\ \hat{\Delta}_{\mathrm{S}}^{\dagger}(z) & \hat{\mathcal{H}}_{\mathrm{h}} \end{bmatrix}, \tag{1}$$

where $\hat{\mathcal{H}}_{\mathrm{e}} = [-\hbar^2/(2m)\, \boldsymbol{\nabla}^2 - \mu]\, \hat{\sigma}_0 - (\Delta_{\mathrm{XC}}/2)\, \Theta(-z)\, (\hat{\mathbf{m}} \cdot \hat{\boldsymbol{\sigma}}) + V_{\mathrm{SC}}\, d_{\mathrm{SC}}\, \hat{\sigma}_0\, \delta(z) + \hat{\mathcal{H}}_{\mathrm{SC}}^{\mathrm{SOC}}\, \delta(z)$ represents the single-electron Hamiltonian and $\hat{\mathcal{H}}_{\mathrm{h}} = -\hat{\sigma}_y\, \hat{\mathcal{H}}_{\mathrm{e}}^*\, \hat{\sigma}_y$ its holelike counterpart ($\hat{\sigma}_0$ and $\hat{\sigma}_i$ indicate the two-by-two identity and the ith Pauli matrix; $\hat{\boldsymbol{\sigma}} = [\hat{\sigma}_x, \hat{\sigma}_y, \hat{\sigma}_z]^\top$ is the vector of Pauli matrices). The F is described within the Stoner model with exchange energy Δ_{XC} and magnetization direction $\hat{\mathbf{m}} = [\cos\Phi, \sin\Phi, 0]^\top$, where Φ is measured with respect to the $\hat{x}$-axis. Following earlier studies [52–56], the ultrathin SC layer is included into our model as a deltalike barrier with height V_{SC} and width d_{SC}; its SOC enters the Hamiltonian [18, 19] $\hat{\mathcal{H}}_{\mathrm{SC}}^{\mathrm{SOC}} =$

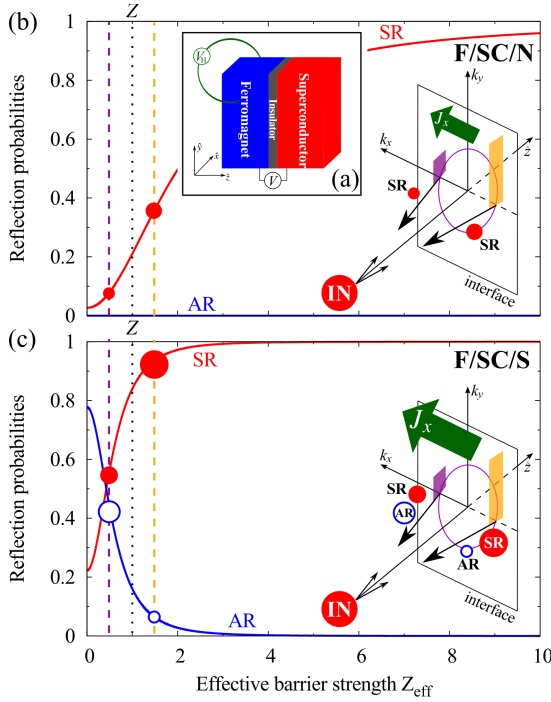* Corresponding author: andreas.costa@physik.uni-regensburg.de

FIG. 1 (Color online). (a) Sketch of the considered F/SC/S junction, using C_{2v} principal crystallographic orientations, $\hat{x} \parallel [110]$, $\hat{y} \parallel [\bar{1}10]$, and $\hat{z} \parallel [001]$. (b) Calculated (zero-bias) *normal state* reflection probabilities for incident spin up electrons (IN) at the SC interface, invoking AR and SR, as a function of $Z_{\text{eff}} = (2mV_{\text{eff}})/(\hbar^2 k_F) = Z - (2\sigma m\alpha k_x)/(\hbar^2 k_F)$ [dimensionless BTK-like barrier parameter for the effective scattering potential in Eq. (2)]; $Z = (2mV_0 d)/(\hbar^2 k_F)$ (see black dashed line for an example) is the usual (spin-independent) barrier strength. Owing to skew reflection, electrons with $k_x < 0$ feel an effectively lowered (dashed violet line) and those with $k_x > 0$ a raised (dashed orange line) barrier; the carrier imbalance (carrier densities are proportional to the size of the red and blue circles) generated via skew SR generates then the transverse Hall current J_x (voltage drop V_{H}). The skew reflection mechanism is schematically illustrated in the inset. (c) Same as in (b), but for the *superconducting* scenario, in which additionally skew AR plays a key role.

$\alpha(k_y \hat{\sigma}_x - k_x \hat{\sigma}_y) - \beta(k_y \hat{\sigma}_x + k_x \hat{\sigma}_y)$, where the first part accounts for SOC of the Rashba type and the second part resembles linearized Dresselhaus SOC [57], both with the effective strengths α and β, respectively. Inside the S electrode, the S pairing potential, $\hat{\Delta}_S(z) = |\Delta_S| \Theta(z)$ ($|\Delta_S|$ is the isotropic energy gap of the S), couples the electron and hole blocks of the BdG Hamiltonian. Note that although writing $\hat{\Delta}_S$ in that way is a rigid approximation, neglecting proximity effects, this approach still yields reliable results for transport calculations [58, 59]. For the sake of simplicity, we further assume the same Fermi levels, μ, and equal effective carrier masses, m, in the F and S.

Assuming translational invariance parallel to the barrier, the solutions of the BdG equation, $\hat{\mathcal{H}}_{\text{BdG}} \Psi^\sigma(\mathbf{r}) = E\,\Psi^\sigma(\mathbf{r})$, can be factorized according to $\Psi^\sigma(\mathbf{r}) = \psi^\sigma(z)\,e^{i(\mathbf{k}_\parallel \cdot \mathbf{r}_\parallel)}$, where $\mathbf{k}_\parallel = [k_x, k_y, 0]^\top$ ($\mathbf{r}_\parallel = [x, y, 0]^\top$) denotes the in-plane momentum (position) vector and $\psi^\sigma(z)$ are the BdG equation's individual solutions for the reduced one-dimensional scattering problem

along $\hat{z}$. The latter account for the different involved scattering processes at the SC interface: incoming electrons with spin σ [$\sigma = +(-)1$ for spin up (down), which effectively indicates a spin parallel (antiparallel) to $\hat{\mathbf{m}}$] may either undergo AR or SR, or may be transmitted as quasiparticles into the S.

Physical picture—Skew AR (& SR). Due to the presence of interfacial SOC, electrons incident on the ultrathin SC are exposed to an effective scattering potential that incorporates besides the usual barrier strength (determined by the barrier's height and width) also the in-plane momentum- and spin-dependent contribution of the SOC. To extract valuable qualitative trends from our model, we first focus on the simple situation in which only Rashba SOC is present ($\alpha > 0$, $\beta = 0$), the F's magnetization is aligned along $\hat{y}$ ($\Phi = \pi/2$), and $k_y = 0$. In this case, the effective scattering potential reads

$$V_{\text{eff}} = V_{\text{SC}}\,d_{\text{SC}} - \sigma\,\alpha\,k_x, \qquad (2)$$

where the first part represents the usual barrier strength and the second the SOC-dependent part. Assuming that SOC is weak and spin-flip scattering becomes negligible, only spin-conserving AR and SR are allowed inside the F, each with certain probabilities. The latter, extracted from an extended Blonder–Tinkham–Klapwijk (BTK) model [60] by substituting the effective scattering potential in Eq. (2) [see the Supplemental Material (SM) [61] for details], are shown for incoming spin up electrons as a function of V_{eff} in Figs. 1(b) and (c), once for the normal state and once for the superconducting junction.

In the first case, AR is completely forbidden, while the probability that the incident electron gets specularly reflected continuously increases with increasing effective scattering potential; note that there is also a finite transmission probability into the right normal state electrode (not shown). For a constant *moderate* barrier height and width (black dashed line) and nonzero Rashba SOC, Eq. (2) suggests that incoming spin up electrons with positive k_x experience a significantly lower barrier (violet dashed line) and thus undergo *skew SR* with a lower probability than those with negative k_x (orange dashed line). The generated spatial charge imbalance in the F must be compensated by a transverse Hall current flow, J_x, along $\hat{x}$. Strictly speaking, the situation gets reversed for incident spin down electrons. Nevertheless, since there are more occupied spin up states, both channels cannot completely cancel and a finite Hall current remains.

If the junction becomes superconducting, AR comes into play. Although the AR probability generally decreases with increasing V_{eff}, the crucial point is that AR involves holes. Consequently, *skew AR* produces simultaneously an electron excess also at negative k_x, and both skew AR and SR act together to noticeably increase the transverse Hall current.

Another important observation relies on the reflection probabilities at large V_{eff}. In both junction scenarios, the SR probabilities approach unity at $V_{\text{eff}} \gg (\hbar^2 k_F)/(2m)$; in the superconducting case much faster than in the normal state. The scattering potential is then mostly determined by the usual barrier height and width, and the spin-dependent contribution only barely impacts V_{eff}. Therefore, both skew reflection and the Hall currents are expected to be strongly damped in the pres-
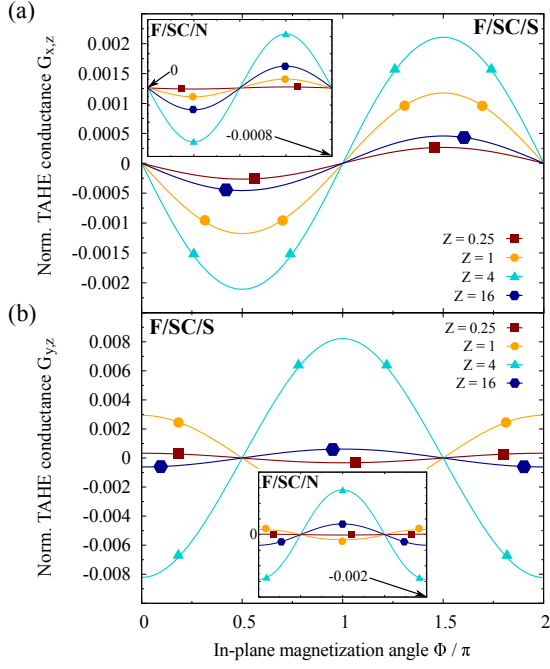
FIG. 2 (Color online). Calculated dependence of the zero-bias TAHE conductances, (a) $G_{x,z}$ and (b) $G_{y,z}$, normalized to Sharvin's conductance, $G_S = (Ae^2k_F^2)/(4\pi^2h)$, on the in-plane magnetization angle Φ, and for various indicated barrier strengths Z; the SOC parameters are $\alpha = 42.3\,\text{eV}\,\text{Å}^2$ and $\beta \approx 19.2\,\text{eV}\,\text{Å}^2 \cdot Z$. The insets show similar normal state calculations, when the S is replaced by a N.

FIG. 3 (Color online). Calculated dependence of the zero-bias TAHE conductances, (a) $G_{x,z}$ and (b) $G_{y,z}$, normalized to G_S, on the in-plane magnetization angle Φ for the same parameters as in Fig. 2. The contributions stemming from SR, spin-flip SR (SR-Flip), and similarly those originating from ARs, are separately resolved.

ence of *strong* barriers, in superconducting even more than in normal-conducting junctions.

TAHE conductances. As a clear fingerprint to experimentally detect skew AR, our qualitative picture suggests a significant enhancement of the superconducting junctions' TAHE conductance, compared to the normal state regime. To evaluate the TAHE conductances along the transverse $\hat{\eta}$-direction ($\eta \in \{x; y\}$), we follow a generalized BTK approach [60], yielding the zero temperature TAHE conductances

$$G_{\eta,z} = -\frac{G_0 A}{8\pi^2} \sum_{\sigma=\pm1} \int d^2\mathbf{k}_{\parallel} \frac{k_\eta}{k_z^\sigma} \left\{ \left[\left| r_e^{\sigma,\sigma}(eV) \right|^2 + \left| r_e^{\sigma,-\sigma}(eV) \right|^2 \right] \right.$$
$$\left. + \left[\left| r_h^{\sigma,-\sigma}(-eV) \right|^2 + \left| r_h^{\sigma,\sigma}(-eV) \right|^2 \right] \right\}, \quad (3)$$

where $G_0 = (2e^2)/h$ abbreviates the conductance quantum, A stands for the cross-section area, $k_z^\sigma = \sqrt{k_F^2(1 + \sigma P) - \mathbf{k}_{\parallel}^2}$ represents the $\hat{z}$-component of the particles' wave vector in the F with spin polarization $P = (\Delta_{XC}/2)/\mu$, and $k_F = \sqrt{2m\mu}/\hbar$ is the Fermi wave vector. The reflection coefficients $r_e^{\sigma,\sigma}$ ($r_e^{\sigma,-\sigma}$) correspond to SR (spin-flip SR), while $r_h^{\sigma,-\sigma}$ ($r_h^{\sigma,\sigma}$) indicate AR (spin-flip AR). Unlike for the (longitudinal) tunneling conductance [60], SR and AR contribute to the Hall conductances with the *same* sign since the specularly reflected electron and the Andreev reflected hole move into opposite transverse directions; the different sign in the transverse velocities gets then compensated by the opposite charge of elec-
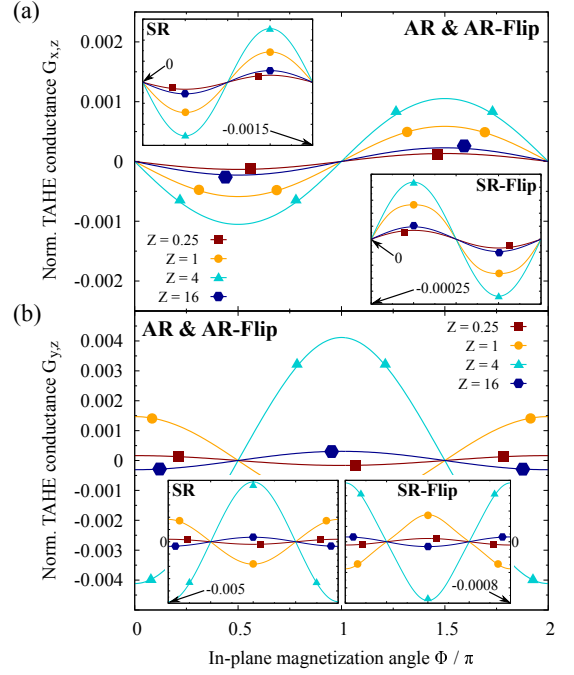
trons and holes. Therefore, the charge imbalances created by skew AR and SR can indeed give rise to individual Hall currents that flow along the same direction, and finally lead to sizable Hall responses in superconducting junctions.

To elaborate on the TAHE conductances' main features, we evaluate Eq. (3) for Fe/GaAs/V like model junctions. The spin polarization in Fe is $P = 0.7$ (Fermi wave vector $k_F \approx 8 \times 10^7\,\text{cm}^{-1}$ [62]), while $|\Delta_S| \sim 1.6\,\text{meV}$ refers to V's gap [62]. The (material-specific) Dresselhaus SOC strength of GaAs can be approximated [19, 63] as $\beta \approx Zk_F\gamma$, with $\gamma \approx 24\,\text{eV}\,\text{Å}^3$ being the cubic Dresselhaus parameter for GaAs [19]. The GaAs barrier's height and width are captured by the dimensionless BTK-like barrier measure $Z = (2mV_{SC}d_{SC})/(\hbar^2k_F)$ (typically, $V_{SC} \sim 0.75\,\text{eV}$ [63], so that $Z = 1$ represents a barrier with thickness $d_{SC} \sim 0.40\,\text{nm}$). Figure 2 shows the dependence of the normalized zero-bias [64] TAHE conductances, $G_{x,z}$ and $G_{y,z}$, on the orientation of the F's magnetization in the F for various barrier strengths Z and the Rashba SOC parameter $\alpha \approx 42.3\,\text{eV}\,\text{Å}^2$, which lies well within the experimentally accessible values [63, 65]. To quantitatively compare the conductance amplitudes, the insets show analogous calculations in the normal-conducting state.

Our simulations reveal all the TAHE conductances' important properties. First, we observe the sin- (cos-like) variation of $G_{x,z}$ ($G_{y,z}$) with respect to the F's magnetization angle. Those dependencies follow from symmetry considerations [61] and unambiguously reflect the junction's magnetoansiotropic transport characteristics [44]. Second, we find
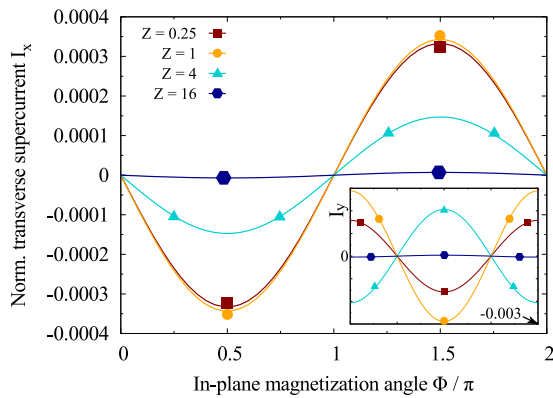
FIG. 4 (Color online). Calculated dependence of the zero-bias transverse supercurrent response, I_x (I_y in the inset), normalized according to $[I_{x(y)}e]/(G_S\pi|\Delta_S|)$, on the in-plane magnetization angle Φ for the same parameters as in Fig. 2.

that skew AR and SR can indeed act together in superconducting junctions, leading to sizable TAHE conductances (& voltages [61]). Specifically, $G_{x,z}$ can be increased by more than one order of magnitude and $G_{y,z}$ still roughly by a factor of four, compared to normal junctions. However, the full physical mechanism is more complicated than our simple picture in Fig. 1, where, we considered one particular combination of in-plane momenta. To obtain the total TAHE conductances, we need to average over all possible configurations [see Eq. (3)], which can—mostly depending on the barrier and Rashba SOC strengths—also reverse the Hall current's direction, observed, for example, in $G_{y,z}$ by increasing Z from $Z = 1$ to $Z = 4$ [61]. Finally, we can confirm the stated connection between the skew reflection mechanism and the TAHE conductances for strong tunneling barriers. As Z increases, V_{eff} is mostly determined by the bare barrier strength itself, see Eq. (2), and the momentum- and spin-dependent SOC asymmetry, responsible for the Hall current generation, gets remarkably suppressed (especially in the superconducting regime). As a result, strong barriers significantly decrease the TAHE conductances.

To resolve AR and SR, Fig. 3 shows their spin-resolved conductance contributions. The spin-flip AR part is not separately shown as its amplitudes are up to two orders of magnitude smaller than those of (spin-conserving) AR. Interestingly, the total TAHE conductance is nearly fully dominated by (spin-conserving) AR and SR; both contributions are comparable in magnitude and have the same signs so that they indeed add up, resulting in sizable TAHE conductances. Since spin-flip SR involves electrons with opposite spin, the effective barrier picture in Fig. 1 gets reversed and the related TAHE conductance contribution changes sign. Nevertheless, this contribution is much smaller than those attributed to spin-conserving skew reflections so that it cannot modify the TAHE conductances' qualitative features.

Supercurrent response. AR is *the* crucial scattering process at metal/S interfaces; it transfers Cooper pairs, converting normal into supercurrents, plays an important role for experimentally quantifying Fs' spin polarization [66], and is also essential for the sizable TAHE conductances in the F of our system. Particularly interesting are the transferred Cooper pairs, which are also exposed to the effective scattering potential and may thus trigger a response in terms of a transverse supercurrent in the S [50]. Within our model, we evaluate the zero-bias supercurrent components, I_η, starting from a generalized Furusaki–Tsukada technique [67]; see the SM [61]. For the considered parameters, we stated that the main skew AR contribution to the TAHE conductance comes from the spin-conserving process. As the latter involves spin-singlet Cooper pairs, composed of electrons with opposite transverse momenta and spins, one could generalize our skew reflection picture to a combined one for the two individual Cooper pair electrons. As a consequence, the induced supercurrents' qualitative features follow the same trends as those of the TAHE conductances in Fig. 2. Figure 4, presenting I_η as a function of the magnetization angle Φ, confirms this expectation: the supercurrent components' dependence on Φ and their orientations (signs) reflect one-by-one the properties of the TAHE conductances in the F. Even the sign change we explored in $G_{y,z}$ when changing Z from $Z = 1$ to $Z = 4$ is (qualitatively) transferred into the supercurrent response I_y. Nevertheless, there is one important difference to the TAHE conductance, concerning the currents' magnitudes. The supercurrent response always results from two single electrons that tunnel into the S, forming a Cooper pair. In order to generate sizable supercurrents, both electrons must simultaneously skew tunnel into the S (mediated by skew AR), which happens less likely at strong barriers than skew tunneling of unpaired electrons. Therefore, the maximal supercurrent amplitudes—several mA for optimal configurations—occur at smaller Z than the maximal TAHE conductance amplitudes in the F.

To conclude, we investigated the intriguing consequences of skew AR and SR at SC interfaces of superconducting tunnel junctions. We predict that the interplay of both skew reflection processes can constructively amplify their effects. Furthermore, also the Cooper pairs transferred into the S via AR cycles are subject to interfacial skew reflections. As a result, both sizable TAHE conductances in the F and characteristically modulating transverse supercurrents in the S are generated, opening new venues for experimental and theoretical studies.

ACKNOWLEDGMENTS

[1] M. Eschrig, Phys. Today **64**, 43 (2011).

[2] J. Linder and J. W. A. Robinson, Nature Phys. **11**, 307 (2015).

[3] E. C. Gingrich, B. M. Niedzielski, J. A. Glick, Y. Wang, D. L. Miller, R. Loloee, W. P. Pratt Jr, and N. O. Birge, Nat. Phys. **12**, 564 (2016).

[4] P. M. Tedrow and R. Meservey, Phys. Rev. Lett. **26**, 192 (1971).

[5] P. M. Tedrow and R. Meservey, Phys. Rev. B **7**, 318 (1973).

[6] R. Meservey and P. M. Tedrow, Phys. Rep. **238**, 173 (1994).

[7] H. Yang, S.-H. Yang, S. Takahashi, S. Maekawa, and S. S. P. Parkin, Nat. Mater. **9**, 586 (2010).

[8] T. Wakamura, H. Akaike, Y. Omori, Y. Niimi, S. Takahashi, A. Fujimaki, S. Maekawa, and Y. Otani, Nat. Mater. **14**, 675 (2015).

[9] D. Beckmann, J. Phys. Condens. Matter **28**, 163001 (2016).

[10] F. S. Bergeret and I. V. Tokatly, Phys. Rev. B **94**, 180502(R) (2016).

[11] C. Espedal, P. Lange, S. Sadjina, A. G. Mal'shukov, and A. Brataas, Phys. Rev. B **95**, 054509 (2017).

[12] J. Linder, M. Amundsen, and V. Risinggård, Phys. Rev. B **96**, 094512 (2017).

[13] J. A. Ouassou, S. H. Jacobsen, and J. Linder, Phys. Rev. B **96**, 094505 (2017).

[14] K.-R. Jeon, C. Ciccarelli, H. Kurebayashi, J. Wunderlich, L. F. Cohen, S. Komori, J. W. A. Robinson, and M. G. Blamire, Phys. Rev. Appl. **10**, 014029 (2018).

[15] X. Montiel and M. Eschrig, Phys. Rev. B **98**, 104513 (2018).

[16] Y. A. Bychkov and E. I. Rashba, J. Phys. C **17**, 6039 (1984).

[17] G. Dresselhaus, Phys. Rev. **100**, 580 (1955).

[18] I. Žutić, J. Fabian, and S. Das Sarma, Rev. Mod. Phys. **76**, 323 (2004).

[19] J. Fabian, A. Matos-Abiague, C. Ertler, P. Stano, and I. Žutić, Acta Phys. Slovaca **57**, 565 (2007).

[20] F. S. Bergeret, A. F. Volkov, and K. B. Efetov, Phys. Rev. Lett. **86**, 4096 (2001).

[21] A. F. Volkov, F. S. Bergeret, and K. B. Efetov, Phys. Rev. Lett. **90**, 117006 (2003).

[22] R. S. Keizer, S. T. B. Goennenwein, T. M. Klapwijk, G. Miao, G. Xiao, and A. Gupta, Nature **439**, 825 (2006).

[23] K. Halterman, P. H. Barsic, and O. T. Valls, Phys. Rev. Lett. **99**, 127002 (2007).

[24] M. Eschrig and T. Löfwander, Nat. Phys. **4**, 138 (2008).

[25] K. Sun and N. Shah, Phys. Rev. B **91**, 144508 (2015).

[26] M. Duckheim and P. W. Brouwer, Phys. Rev. B **83**, 054513 (2011).

[27] F. S. Bergeret and I. V. Tokatly, Phys. Rev. Lett. **110**, 117003 (2013).

[28] F. S. Bergeret and I. V. Tokatly, Phys. Rev. B **89**, 134517 (2014).

[29] S. H. Jacobsen and J. Linder, Phys. Rev. B **92**, 024501 (2015).

[30] J. Nilsson, A. R. Akhmerov, and C. W. J. Beenakker, Phys. Rev. Lett. **101**, 120403 (2008).

[31] S.-P. Lee, J. Alicea, and G. Refael, Phys. Rev. Lett. **109**, 126403 (2012).

[32] S. Nadj-Perge, I. K. Drozdov, J. Li, H. Chen, S. Jeon, J. Seo, A. H. MacDonald, B. A. Bernevig, and A. Yazdani, Science **346**, 602 (2014).

[33] E. Dumitrescu, B. Roberts, S. Tewari, J. D. Sau, and S. Das Sarma, Phys. Rev. B **91**, 094505 (2015).

[34] R. Pawlak, M. Kisiel, J. Klinovaja, T. Meier, S. Kawai, T. Glatzel, D. Loss, and E. Meyer, npj Quantum Inf. **2**, 16035 (2016).

[35] M. Ruby, B. W. Heinrich, Y. Peng, F. von Oppen, and K. J. Franke, Nano Lett. **17**, 4473 (2017).

[36] G. Livanas, M. Sigrist, and G. Varelogiannis, Sci. Rep. **9**, 6259 (2019).

[37] E. Hall, London, Edinburgh, Dublin Philos. Mag. J. Sci. **12**, 157 (1881).

[38] P. Wölfle and K. Muttalib, Ann. Phys. **15**, 508 (2006).

[39] N. Nagaosa, J. Phys. Soc. Japan **75**, 042001 (2006).

[40] N. A. Sinitsyn, J. Phys. Condens. Matter **20**, 023201 (2008).

[41] N. Nagaosa, J. Sinova, S. Onoda, A. H. MacDonald, and N. P. Ong, Rev. Mod. Phys. **82**, 1539 (2010).

[42] A. Vedyayev, N. Ryzhanova, N. Strelkov, and B. Dieny, Phys. Rev. Lett. **110**, 247204 (2013).

[43] A. V. Vedyayev, M. S. Titova, N. V. Ryzhanova, M. Y. Zhuravlev, and E. Y. Tsymbal, Appl. Phys. Lett. **103**, 032406 (2013).

[44] A. Matos-Abiague and J. Fabian, Phys. Rev. Lett. **115**, 056602 (2015).

[45] T. H. Dang, H. Jaffrès, T. L. Hoai Nguyen, and H.-J. Drouhin, Phys. Rev. B **92**, 060403(R) (2015).

[46] T. H. Dang, D. Quang To, E. Erina, T. Hoai Nguyen, V. Safarov, H. Jaffrès, and H.-J. Drouhin, J. Magn. Magn. Mater. **459**, 37 (2018).

[47] M. Y. Zhuravlev, A. Alexandrov, L. L. Tao, and E. Y. Tsymbal, Appl. Phys. Lett. **113**, 172405 (2018).

[48] V. V. Rylkov, S. N. Nikolaev, K. Y. Chernoglazov, V. A. Demin, A. V. Sitnikov, M. Y. Presnyakov, A. L. Vasiliev, N. S. Perov, A. S. Vedeneev, Y. E. Kalinin, V. V. Tugushev, and A. B. Granovsky, Phys. Rev. B **95**, 144202 (2017).

[49] Conventional *skew scattering* actually refers to momentum- and spin-dependent scattering of spin-polarized charge carriers on magnetic impurities. To clearly differentiate between that and our reflection-based mechanism (which does not require the presence of impurities at all), we rely on the term *skew reflection*.

[50] S. Mironov and A. Buzdin, Phys. Rev. Lett. **118**, 077001 (2017).

[51] P. G. De Gennes, *Superconductivity of Metals and Alloys* (Addison Wesley, Redwood City, 1989).

[52] M. J. M. de Jong and C. W. J. Beenakker, Phys. Rev. Lett. **74**, 1657 (1995).

[53] I. Žutić and O. T. Valls, Phys. Rev. B **60**, 6320 (1999).

[54] I. Žutić and O. T. Valls, Phys. Rev. B **61**, 1555 (2000).

[55] A. Costa, P. Högl, and J. Fabian, Phys. Rev. B **95**, 024514 (2017).

[56] A. Costa, J. Fabian, and D. Kochan, Phys. Rev. B **98**, 134511 (2018).

[57] Higher-order SOC terms can be neglected since the main current contributions come from states with small k_x and k_y [63].

[58] K. K. Likharev, Rev. Mod. Phys. **51**, 101 (1979).

[59] C. W. J. Beenakker, Rev. Mod. Phys. **69**, 731 (1997).

[60] G. E. Blonder, M. Tinkham, and T. M. Klapwijk, Phys. Rev. B **25**, 4515 (1982).

[61] See Supplemental Material at [link], including Refs. [16–19, 44, 47, 48, 51–56, 60, 63, 65, 67–74], for more details.

[62] I. Martínez, P. Högl, C. González-Ruano, J. P. Cascales, C. Tiusan, Y. Lu, M. Hehn, A. Matos-Abiague, J. Fabian, I. Žutić, and F. G. Aliev, (submitted) (2018), arXiv:1812.08090.

[63] A. Matos-Abiague and J. Fabian, Phys. Rev. B **79**, 155303 (2009).

[64] Experimental measurements of the TAHE response in the F simultaneously detect a contribution stemming from conven-

tional anomalous Hall effects. To separate both parts, one could exploit the TAHE contribution's unique voltage dependence [61].

[65] J. Moser, A. Matos-Abiague, D. Schuh, W. Wegscheider, J. Fabian, and D. Weiss, Phys. Rev. Lett. **99**, 056601 (2007).

[66] R. J. Soulen, M. S. Osofsky, B. Nadgorny, T. Ambrose, P. Broussard, S. F. Cheng, J. Byers, C. T. Tanaka, J. Nowack, J. S. Moodera, G. Laprade, A. Barry, and M. D. Coey, J. Appl. Phys. **85**, 4589 (1999).

[67] A. Furusaki and M. Tsukada, Solid State Commun. **78**, 299 (1991).

[68] P. Högl, A. Matos-Abiague, I. Žutić, and J. Fabian, Phys. Rev. Lett. **115**, 116601 (2015); Phys. Rev. Lett. **115**, 159902(E) (2015).

[69] W. L. McMillan, Phys. Rev. **175**, 559 (1968).

[70] J. Nitta, T. Akazaki, H. Takayanagi, and T. Enoki, Phys. Rev. Lett. **78**, 1335 (1997).

[71] T. Koga, J. Nitta, T. Akazaki, and H. Takayanagi, Phys. Rev. Lett. **89**, 046801 (2002).

[72] L. Chen, M. Gmitra, M. Vogel, R. Islinger, M. Kronseder, D. Schuh, D. Bougeard, J. Fabian, D. Weiss, and C. Back, Nat. Electron. **1**, 350 (2018).

[73] D. C. Giancoli, *Physics*, 4th ed. (Prentice Hall, 1995).

[74] X. Wang, J. R. Yates, I. Souza, and D. Vanderbilt, Phys. Rev. B **74**, 195118 (2006); Phys. Rev. B **76**, 169902(E) (2007).